Particle transport velocity correction for complex boundaries in the Finite Volume Particle Method

Particle transport velocity correction for complex boundaries in the Finite Volume Particle Method

Maryrose McLoone, Mohsen H. Moghimi, and Nathan J. Quinlan
Mechanical Engineering, CÚRAM Centre for Research in Medical Devices, and Biomechanics Research Centre
National University of Ireland Galway
Galway, Ireland
m.mcloone1@nuigalway.ie

***Abstract*—Particle methods such as smoothed particle hydrodynamics (SPH) and the finite volume particle method (FVPM) can suffer from strongly non-uniform and anisotropic particle distributions when purely Lagrangian particle motion is employed, resulting in numerical error. In this paper, we evaluate two Arbitrary Lagrangian Eulerian (ALE) particle transport velocity corrections for FVPM, adapted from SPH methods with a new treatment for boundaries without fictitious particles. The methods are tested on Taylor-Green flow, lid driven cavity flow (with additional complex geometry), oscillating free-surface flow, and dam-break free-surface flow. Results show that the correction formulation can maintain good particle distribution with nearly Lagrangian particle motion. The new boundary treatment is found to be effective for varying spatial resolution and complex geometry over a range of scales, without fictitious boundary particles and without parameter tuning.**

I. INTRODUCTION

The finite volume particle method (FVPM) is a particle method based on the meshless framework and kernel gradient operators of smoothed particle hydrodynamics (SPH), with finite-volume concepts of fluxes and interface area for conservative particle-particle and particle-boundary interactions [1–4]. FVPM, like SPH (particularly in modified higher-order formulations [5]), is susceptible to non-uniform and anisotropic particle distribution due to Lagrangian particle transport. In this paper we present a scheme for particle transport velocity correction (or shifting) in the FVPM, with a novel approach for walls.

Nestor *et al*. [6] proposed a small adjustment to the Lagrangian particle transport velocity to improve particle distribution, exploiting the Arbitrary Lagrangian Eulerian (ALE) nature of the FVPM method:

$$\dot{\mathbf{x}}_i = \mathbf{u}_i + \dot{\mathbf{x}}_i' , \tag{1}$$

where $\dot{\mathbf{x}}_i$ is the particle transport velocity, $\mathbf{u}_i$ is the fluid velocity and $\dot{\mathbf{x}}_i'$ is the particle transport velocity correction. The intrinsic ALE formulation of FVPM enables interparticle fluxes due to the non-Lagrangian component, $\dot{\mathbf{x}}_i'$, to be correctly accounted for. This helps to preserve the advantages of (nearly) Lagrangian particle transport while also maintaining the quality of the particle distribution. Nestor *et al*. [6] used an inverse-square interparticle repulsive effect to determine $\dot{\mathbf{x}}_i'$. Jahanbakhsh *et al*. [7] developed an alternative form. In SPH, the particle shifting approach was developed by Xu *et al*. [8], and further refined by Lind *et al*. [9], Skillen *et al*. [10], and Mokos *et al*. [11], based on Fickian diffusion of particles. Oger *et al*. [12] formulated a similar scheme in terms of velocity correction rather than a displacement shift.

Most versions of SPH employ fictitious boundary particles, and so particle distribution correction schemes operate near boundaries with little or no modification. Since FVPM does not require fictitious particles, correction methods may behave asymmetrically at boundaries. In this work, we present an adaptation of the approaches of Lind *et al*. [9] and Oger *et al*. [12] from SPH to the FVPM framework, with a novel treatment for boundaries. In these methods the particle redistribution is dependent on the gradient of a kernel-like function. In the new FVPM adaptation, the boundary contribution to the ALE particle transport velocity correction is computed as an approximation of a field of particles outside the boundary, without explicitly computing the position of fictitious particles.

II. EXISTING PARTICLE REDISTRIBUTION METHODS

A. Fickian diffusion method in SPH

The particle shifting method developed by Lind *et al*. [9] has shown success in achieving a uniform and isotropic particle distribution in SPH. The method closely follows Fick's law, where the diffusive flux of particles is a function of the concentration (particle number density) gradient:

$$\dot{\mathbf{x}}_{i,f}' = -0.5\frac{h^2}{\Delta t}\left(\frac{\sum_{\mathrm{j}} \nabla W_{ij} V_j}{\sum_{\mathrm{j}} W_{ij} V_j}\right), \tag{2}$$

where h is the particle smoothing length, Δt is the time step, j denotes the neighbours of particle i, W_{ij} is the particle kernel, and V_j is the volume of particle j. This method was originally formulated as a particle shift [9], but is expressed here in terms of a velocity, to allow easy comparison with other methods.

The value of diffusivity D is limited by $D \leq 0.5h^2/\Delta t$, which is based on a von Neumann stability analysis of the advection–diffusion equation [9]. For most test cases, Lind *et al*. [9] select a diffusion coefficient at the upper limit, i.e. $D = 0.5h^2/\Delta t$, as in (2) above.

B. Kernel gradient method in SPH

Similarly, Oger *et al*. [12] proposed a particle shifting velocity based on the sum of the kernel gradients evaluated at a particle's neighbours. This method does not depend on a

diffusion coefficient, but instead the velocity correction scales with a reference physical velocity U as follows:

$$\dot{\mathbf{x}}'_{i,k} = -2Uh\sum_{\mathrm{j}} \nabla W^*_{ij} V_{0j}\,, \tag{3}$$

where V_{0j} is the initial volume of particle j. W^*_{ij} denotes a kernel with enlarged support radius of $2\Delta x$, where Δx is the initial particle spacing, rather than $2h$. This correction velocity is capped at 25% of the local fluid velocity to maintain nearly Lagrangian particle motion.

C. Particle repulsion in FVPM

In FVPM, Nestor *et al*. [6] developed a particle velocity correction based on the inverse of the particle spacing, in which particles experience a repulsive effect based on their proximity to each other. A similar repulsive correction is added as a function of distance to the boundary, which is modelled without fictitious particles.

This method is successful in maintaining uniform particle distribution and enables some challenging test cases, but has coefficients which are resolution-dependent and must be tuned separately for interparticle and boundary-particle repulsion effects. Furthermore, for particles interacting with multiple boundary segments, each segment contributes equally and additively to the velocity correction. This causes difficulty at corners and near curved geometry represented by a series of small linear segments.

III. New scheme for particle transport velocity correction in FVPM

The objective of this work is to develop a particle transport velocity correction method that is robust under varying resolution and takes advantage of FVPM's purely geometric representation of boundaries, without fictitious particles. The absence of boundary particles requires a new scheme for boundaries, which can then be used with either the kernel gradient or Fickian approaches adapted from SPH.

A. Boundaries

We compute the boundary contribution to the correction velocity by approximating the effect of a field of particles which is continuous across the boundary, as shown in Fig. 1 (although no particles are positioned outside the boundary). The distance r_{ib} is the perpendicular distance from particle i to the boundary plus $\Delta x/2$. This distance is used to evaluate kernel gradients. L_b is the length of the boundary segment covered by the particle support. The term $L_b/\Delta x$ is the number of particles which could be distributed along the length of the boundary segment, and acts as a weighing factor on the effect of a single neighbour particle. This approach is compatible with either of the SPH approaches, as explained below.

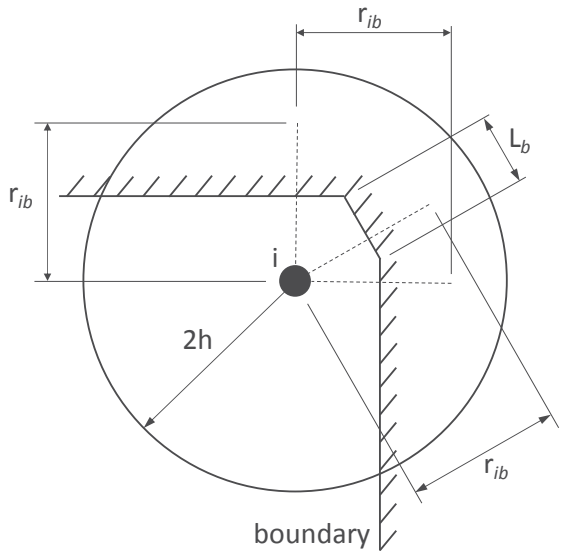

Figure 1. Computation of boundary distance, r_{ib}, applied to three boundary segments.

B. Kernel gradient method applied to FVPM

The kernel gradient particle shifting method of Oger *et al*. [12] is adapted here for FVPM. As in the kernel gradient method, the particle-particle contribution to the particle transport velocity correction is based on the sum of the kernel gradients evaluated at a particle's neighbours:

$$\dot{\mathbf{x}}'_p = \sum_{\mathrm{j}} \nabla W_{ij}\, V_{0j}\,, \tag{4}$$

where the particle volume, V_{0j}, is set as the nominal volume, Δx^2.

The boundary segments contribute an additional correction

$$\dot{\mathbf{x}}'_b = -\sum_{\mathrm{b}} \frac{L_b}{\Delta x} \nabla W_{ib} V_{0i}\ , \tag{5}$$

where the kernel W_{ib} is evaluated at a distance $r_{ib,}$ as discussed above.

From (4) and (5) the particle transport velocity correction method for FVPM, adapted from the kernel gradient method with the new formulation for boundary effects, is given as:

$$\dot{\mathbf{x}}'_i = \begin{cases} -2Uh\left(\dot{\mathbf{x}}'_p + \dot{\mathbf{x}}'_b\right) & \text{if } |\dot{\mathbf{x}}'_i| < 0.25U \\ -0.25U\dfrac{\dot{\mathbf{x}}'_p + \dot{\mathbf{x}}'_b}{\left|\dot{\mathbf{x}}'_p + \dot{\mathbf{x}}'_b\right|} & \text{otherwise.} \end{cases} \tag{6}$$

Whereas Oger *et al*. [12] limited $\dot{\mathbf{x}}'_i$ to 25% of the local velocity, here we impose a cap of 25% of the reference velocity, U. This modification allows particle distribution to be improved in regions of very low velocity.

C. Fickian diffusion method applied to FVPM

The Fickian SPH particle shifting approach is applied in a similar manner. A boundary term is added to (2) to give a particle shifting velocity of

$$\dot{\mathbf{x}}_i' = -0.5\frac{h^2}{\Delta t}\left(\frac{\sum_j \nabla W_{ij} V_j}{\sum_j W_{ij} V_j} + \frac{L_b}{\Delta x}\frac{\sum_j \nabla W_{ib} V_i}{\sum_j W_{ib} V_i}\right). \quad (7)$$

This shifting velocity was also capped at 25% of the reference velocity in the present work, to simplify comparison between the methods.

Comparison of (4–6) and (7) shows that the methods are very similar. Both use $\sum_j \nabla W_{ij} V_j$ as a sensor of non-uniformity of particle distribution. Lind *et al.* [9] interpret this as the gradient of particle concentration (weighted by volume, which is constant in their original incompressible formulation). The methods differ in the use of the normalising term $\sum_j W_{ij} V_j$, which is an SPH estimate of particle concentration, weighted by particle volume. However, this is approximately 1 and so does not affect the order of magnitude of the result.

More significantly, the kernel gradient and Fickian methods have different scaling coefficients of $2Uh$ and $h^2/(2\Delta t)$, respectively. Since $h/\Delta t$ is determined by a CFL condition, it is on the order of physical velocity U in incompressible applications for which the Fickian approach was developed [9]. The two scaling factors are then similar. On the other hand, in the weakly compressible test cases in this paper, $h/\Delta t$ is on the order of the sound speed, and the scale of resulting velocity correction is much larger in the Fickian formulation. In effect, the sound speed becomes the reference scale for the velocity correction.

D. Free-surface correction

At a free surface, we do not apply the particle transport velocity correction as we would for internal particles, since Lagrangian particle motion is necessary to track the free surface. A particle is determined to be a free-surface particle if the sum of the interparticle area, $\boldsymbol{\beta}_{ij}$, is non-zero. $\boldsymbol{\beta}_{ij}$ is closely analogous to the intercell area vector in the finite-volume method. The sum $\sum \boldsymbol{\beta}_{ij}$ for a particle i on the surface is normal to the free surface. Therefore, following Jahanbakhsh *et al.* [7], we apply a correction only in the plane normal to $\sum \boldsymbol{\beta}_{ij}$, suppressing non-Lagrangian motion normal to the free surface.

$$\dot{\mathbf{x}}_{fs}' = \dot{\mathbf{x}}_i' - \left(\dot{\mathbf{x}}_i' \cdot \frac{\sum_j \boldsymbol{\beta}_{ij}}{\left|\sum_j \boldsymbol{\beta}_{ij}\right|}\right)\left(\frac{\sum_j \boldsymbol{\beta}_{ij}}{\left|\sum_j \boldsymbol{\beta}_{ij}\right|}\right). \quad (8)$$

Numerical voids can appear in the domain and create non-physical free-surfaces. The method proposed by Moghimi and Quinlan [13] is used to differentiate between physical and non-physical free-surfaces on the basis that new isolated free surfaces should never appear. The tangential free-surface particle velocity correction is applied to physical real surfaces and the standard correction is applied to non-physical free-surfaces.

IV. Numerical Tests

A number of test cases have been simulated with the proposed kernel gradient and Fickian diffusion particle transport velocity correction methods as adapted for FVPM. For all simulations, the fluid is modelled as weakly compressible with the Tait equation of state. The cubic spline kernel is used for particle transport velocity correction, as discussed above. Other details of the FVPM formulation follow [4] and [6].

A. Taylor-Green Flow

The Taylor-Green flow consists of decaying vortices in a square domain with periodic boundaries. The stagnation points in the flow lead to undesirable particle clustering when using purely Lagrangian particle motion. The particle transport velocity correction described in section III is applied to a Taylor-Green flow for a square domain of size $L \times L$, with Reynolds number $\mathrm{Re}_L = 100$, and Mach number $M = 0.1$. This flow was modelled with 100×100 particles. A smoothing length of $h = 0.8\Delta x$ was used, where Δx is the initial particle spacing.

In Fig. 2 it can be seen that at time $t^* = tU/L = 0.2$, for both correction methods, the particle distribution is uniform, and the pressure distribution is smooth. At this time with a purely Lagrangian model, anisotropic particle distributions form, causing large errors [12]. The results achieved with the particle correction methods agree well with each other.

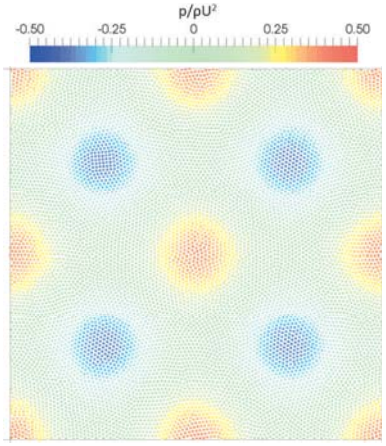

(a) Fickian diffusion method for particle transport velocity

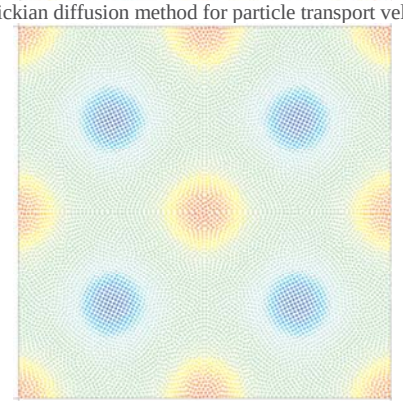

(b) Kernel gradient method for particle transport velocity

Figure 2. Taylor-Green flow: comparison of pressure, for $\mathrm{Re}_L = 100$, 100×100 particles, at $tU/L = 0.2$.

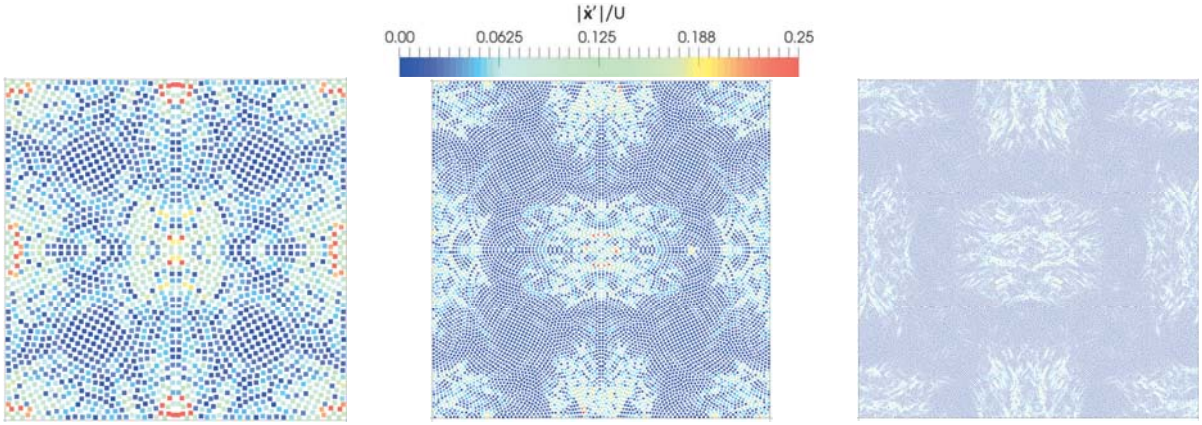

(e) $L/\Delta x = 50$ (e) $L/\Delta x = 100$ (f) $L/\Delta x = 200$

Figure 3. Taylor-Green flow: Resolution study - comparison of particle velocity correction magnitude for the kernel gradient method for particle transport velocity, for $L/\Delta x = \{50, 100, 200\}$, for $Re_L = 100$, at $tU/L = 0.2$.

A resolution study was carried out to determine the effect of resolution on the proposed FVPM kernel gradient particle transport velocity correction. As shown in Fig. 3, the particle velocity correction magnitude shows areas of high correction near the stagnation points. This is expected as there is a high velocity gradient in these areas due to the flow around the stagnation points. The areas of high and low velocity correction magnitude remain the same for each resolution in Fig. 3. This shows that resolution has no major effect on the velocity correction magnitude and therefore the method does not require any tuning for varying resolution.

B. Lid-driven cavity

The lid-driven cavity geometry was set up as a square of size $L \times L$. The left ($x/L = 0$), right ($x/L = 1$), and bottom ($y/L = 0$) walls have a no-slip boundary condition with a velocity of $U_x = U_y = 0$. The top ($y/L = 1$) wall velocity is a no-slip wall with a velocity of $U_x = U$. The simulation was run with a Reynolds number $Re_L = 1000$ and Mach number $M = 0.1$. More complex geometry was introduced with a baffle and a segmented rough boundary, as shown in Fig. 4. This is representative of a curved wall modelled with small segments. The simulation resolution was 100×100 particles with $h = 0.8\Delta x$. In this case the small boundary segments are of length $(1.4)h$, less than the particle support radius. The Fickian diffusion and kernel gradient methods were compared with results for no correction (Lagrangian motion).

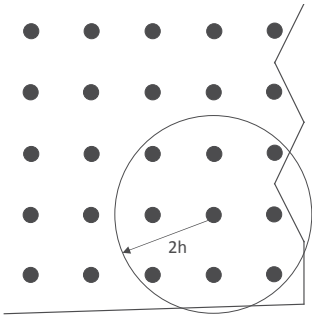

Figure 4. Particle kernel around complex boundary in the lid-driven cavity geometry for $h/\Delta x = 0.8$.

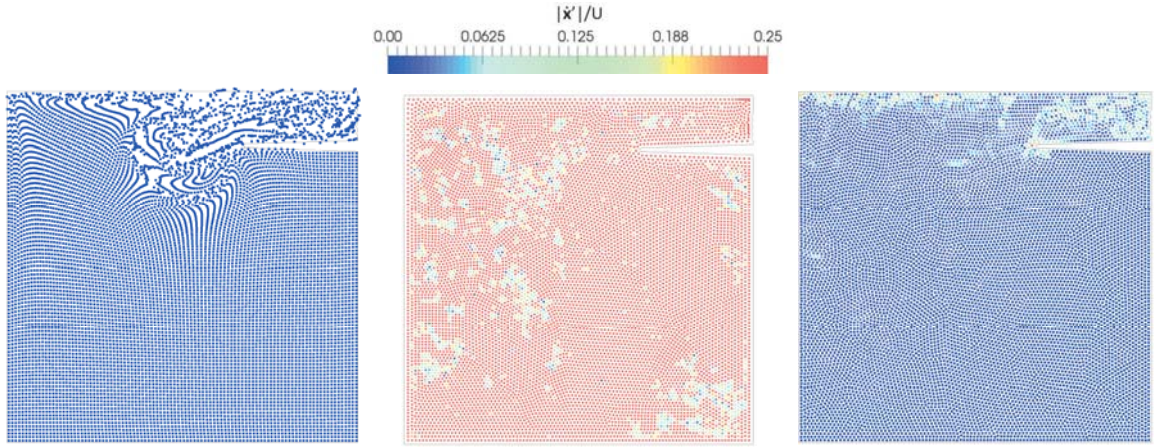

(a) Lagrangian motion, $tU/L = 2.3$ (b) Fickian diffusion method for particle transport velocity, $tU/L = 10$ (c) Kernel gradient method for particle transport velocity, $tU/L = 10$

Figure 5. Lid-driven cavity with complex boundaries: comparison of particle velocity correction magnitude, for $Re_L = 1000$, 100×100 particles.

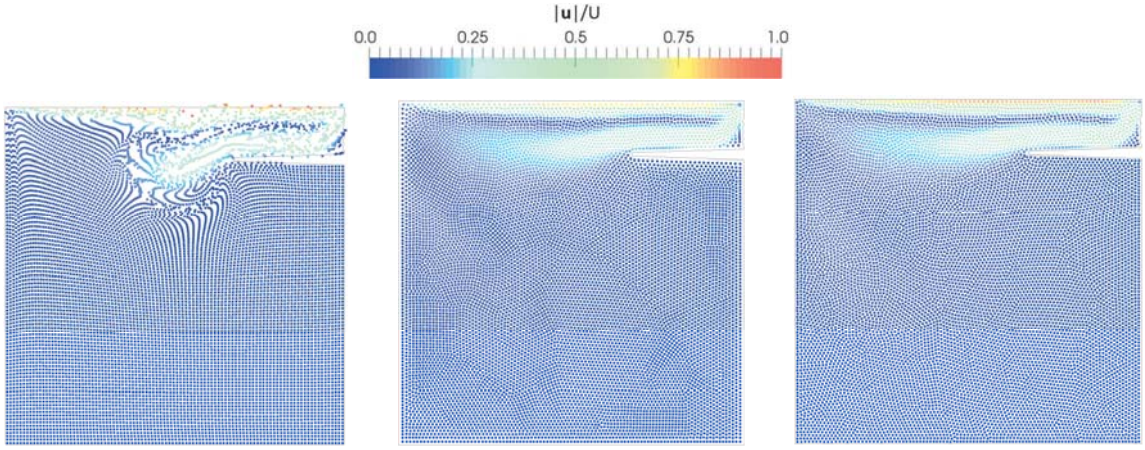

(a) Lagrangian motion, $tU/L = 2.3$ (b) Fickian diffusion method for particle transport velocity, $tU/L = 10$ (c) Kernel gradient method for particle transport velocity, $tU/L = 10$

Figure 6. Lid-driven cavity with complex boundaries: comparison of velocity magnitude, for Re_L =1000, 100×100 particles.

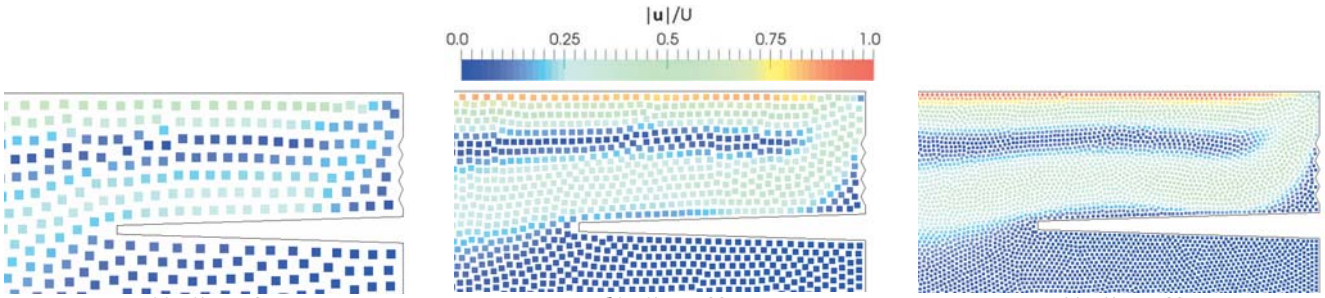

(a) $L/\Delta x = 50$ (b) $L/\Delta x = 100$ (c) $L/\Delta x = 200$

Figure 7. Lid-driven cavity resolution study - comparison of velocity correction magnitude around geometric details, with the kernel gradient method for particle transport velocity, for $Re_L = 1000$, at $tU/L = 10$.

The results in Fig. 5 show the particle velocity correction magnitude for purely Lagrangian motion, the FVPM Fickian diffusion correction method, and the FVPM kernel gradient correction method. The purely Lagrangian method failed at $tU/L = 2.3$ due to poor particle distribution. In the kernel gradient method, the correction is highest along the upper wall, due to the large velocity gradient in this area caused by upper wall velocity. There is also a large particle velocity correction magnitude around the tip of the baffle due to the sharp change in direction. Correction magnitude was very high for the Fickian method, and in many cases up to the limit of 0.25 U. This is expected in these weakly compressible tests, from the examination of scaling in section III above. Therefore, most tests were conducted with the kernel gradient method. In this method, the velocity correction scales with the reference physical velocity U, and it is therefore less sensitive to numerical choices such as the compressibility model.

In Fig. 6 (a) the Lagrangian particle transport field has resulted in particle clustering and large voids in the domain. In Fig. 6 (b) and (c) the Fickian diffusion and kernel gradient methods have resulted in a smooth particle distribution. The fluid velocity magnitude results for both correction methods are in agreement.

A resolution study was conducted with the proposed FVPM kernel gradient particle transport velocity correction method, with resolutions of $L/\Delta x = \{50, 100, 200\}$. In Fig. 7 there is a uniform distribution of particles around the detailed geometry. With increasing resolution, particles are located closer to the wall, and the maximum fluid velocity tends to the wall velocity. At the highest resolution ($L/\Delta x = 200$), particle size is similar to the size of the small geometric features, and particles move into the recesses in the wall. As shown in Fig. 8, good particle distribution is maintained for long times ($tU/L = 100$).

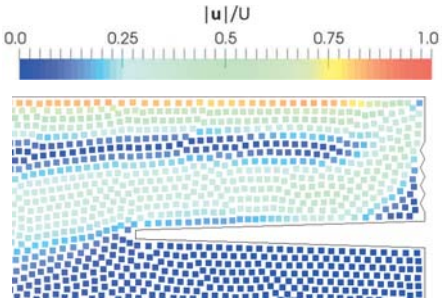

Figure 8. Lid-driven cavity with complex boundaries: velocity magnitude around geometric details, with the kernel gradient method for particle transport velocity, for $Re_L = 1000$, 100×100 particles, at $tU/L = 100$.

C. *Liquid in an oscillating tank*

Liquid in an oscillating tank is a difficult test case due to high acceleration and pressure gradient, with strong acoustic waves. For this test case the geometry is a tank of width L, filled with fluid to a height $0.5L$. The boundaries are no-slip walls. The flow is modelled in the reference frame of the tank by applying an oscillatory body force on the fluid in the y direction. The oscillation amplitude is $A/L = 2.5\times10^{-3}$. The Reynolds number is $Re_L = \rho A\omega L/\mu = 1003$ and the Mach number is $M=A\omega/c_0=0.02$, where ω is the angular frequency and c_0 is the reference speed of sound. 25×50 particles are used with a smoothing length of $h=0.8\Delta x$. Both particle transport velocity correction methods are compared with Lagrangian motion.

The results in Fig. 9 and 10 (a) show that when no correction is applied, the particle distribution becomes irregular. In Fig 9 (b) and (c), when the Fickian diffusion or kernel gradient methods are applied the particles remain in nearly uniform distribution. The pressure distribution is similar in the two methods. As shown in Fig. 10, the correction is highest at that time at the lower wall, and low in the rest of the domain. The pressure distribution plots in Fig.11 show that a compression wave forms from the bottom wall, moves up to the free-surface, and back down in one cycle, as expected.

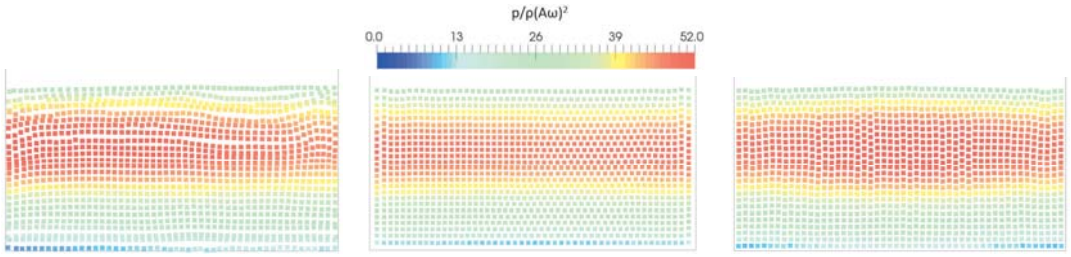

(a) Lagrangian motion (b) Fickian diffusion method for particle transport velocity (c) Kernel gradient method for particle transport velocity

Figure 9. Liquid in an oscillating tank: pressure distribution at $t^* = t\omega/(2\pi) = 100$.

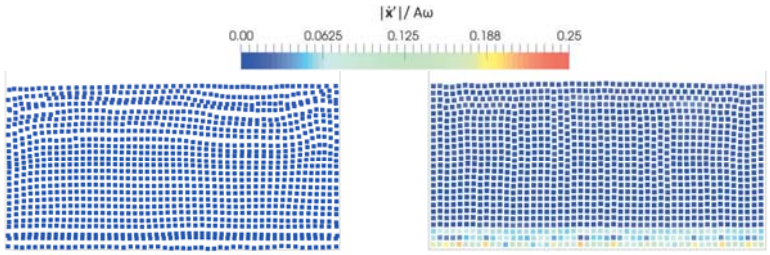

(a) Lagrangian motion (b) Kernel gradient method for particle transport velocity

Figure 10. Liquid in an oscillating tank: particle velocity correction at $t^* = t\omega/(2\pi) = 100$.

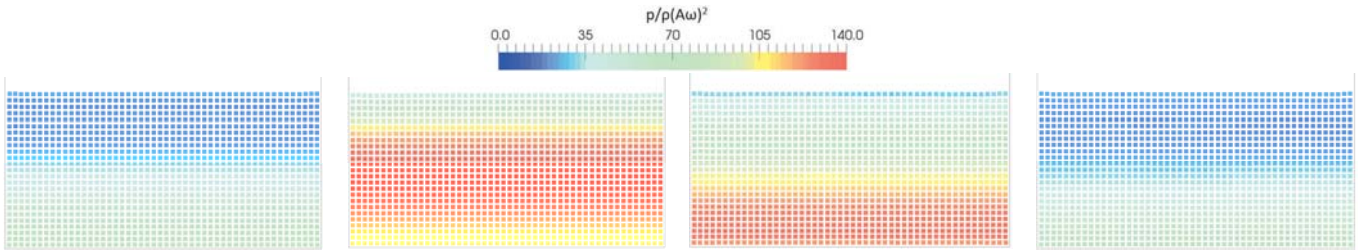

(a) $t\omega/(2\pi) = 2.4$ (b) $t\omega/(2\pi) = 2.6$ (c) $t\omega/(2\pi) = 2.95$ (d) $t\omega/(2\pi) = 3.1$

Figure 11. Liquid in an oscillating tank: pressure distribution during one cycle, with the kernel gradient method for particle transport velocity.

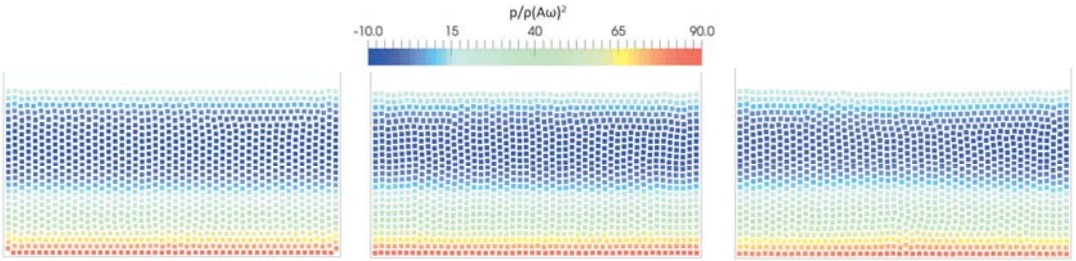

(a) $t\omega/(2\pi) = 100$ (b) $t\omega/(2\pi) = 140$ (c) $t\omega/(2\pi) = 200$

Figure 12. Liquid in an oscillating tank: pressure distribution with the kernel gradient method for particle transport velocity.

Results in Fig.12 show that the particles remain in a uniform distribution for up to 200 cycles, and the pressure distribution remains smooth in space and periodic in time.

D. Dam-break

The dam-break experiment of Lobovský *et al*. [14] was modelled with inviscid fluid and free-slip walls with the kernel gradient particle transport correction method applied to FVPM. A volume of water, of height H and length $2H$, is initially behind a gate, which is removed at constant velocity. The initial particle spacing is set to $H/\Delta x = 30$ with a smoothing length of $h = 0.6\Delta x$. The simulation was run for a Mach number $M = \sqrt{gH}/c_0 = 0.05$.

The results in Fig. 13 show smooth pressure distribution at the time of gate release, run-up on the downstream wall, and the secondary wave.

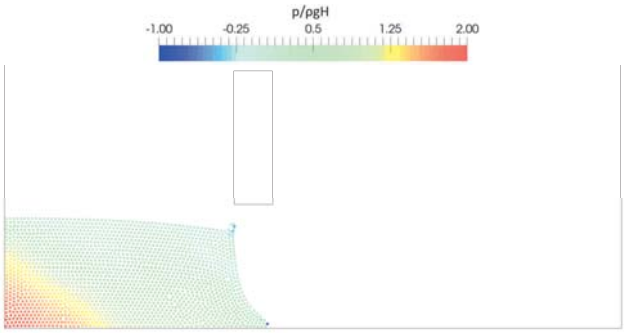

(a) $tU/H = 0.5$, gate release

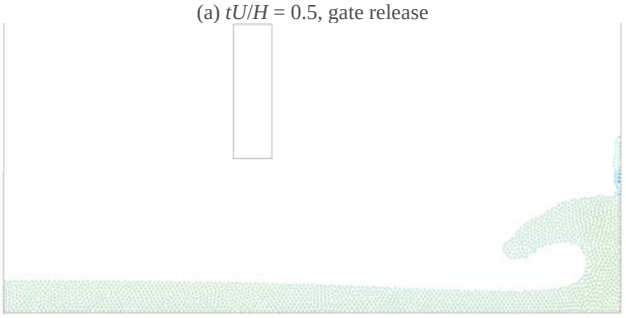

(b) $tU/H = 6$, gate removed

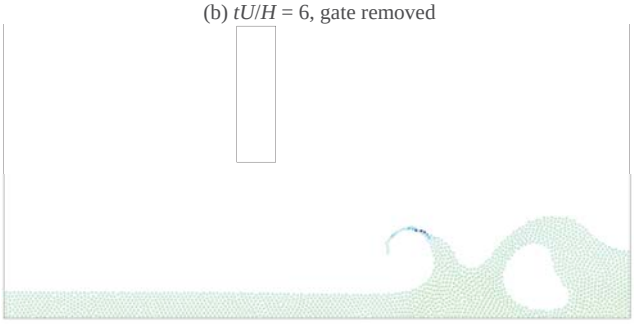

(c) $tU/H = 7$, gate removed

Figure 13. Dam-break: pressure distribution, with the kernel gradient method for particle transport velocity, where $U = \sqrt{gH}$, for $M = 0.05$, $H/\Delta x = 30$.

The plot in Fig. 14 shows the particle correction velocity, nondimensionalised by the reference velocity $\sqrt{gH}$. Some particles experience high correction velocity in the region of wave breaking. This is expected as the velocity gradient is high in this area.

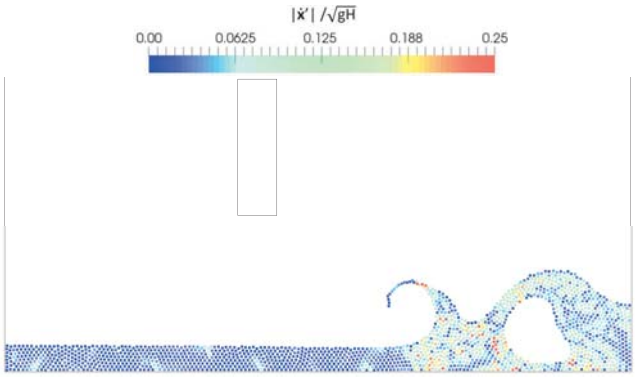

Figure 14. Dam-break: particle transport velocity correction magnitude at $tU/H = 7$, with the kernel gradient method for particle transport velocity, for $M = 0.05$, $H/\Delta x = 30$.

V. CONCLUSION

In this paper, a method has been presented for calculation of ALE particle transport velocity in FVPM to maintain uniform particle distributions. The correction method is based on particle-particle interactions in the SPH literature [9,12], with a new scheme to adapt these methods to FVPM boundaries without fictitious particles. The method requires no parameter tuning, unlike the previous scheme for FVPM with particle-free boundaries [6].

The method was tested in Taylor-Green flow, lid-driven cavity flow and oscillating and dam-break free-surface flow. The kernel gradient particle transport velocity correction method maintained uniform particle distribution in tests across a range of spatial resolution and for long-duration flows in the steady and oscillatory test cases.

Results of the Fickian diffusion method, when tested, were similar. The two methods are essentially similar, differing mainly in their scaling coefficient. However, the Fickian method produced much higher velocity correction in most cases. This is due to its scaling coefficient designed for incompressible applications, but applied here for a weakly compressible fluid.

ACKNOWLEDGEMENT

Maryrose McLoone is funded by a Government of Ireland Postgraduate Research Scholarship from the Irish Research Council.

REFERENCES

[1] D. Hietel, K. Steiner, J. Struckmeier, “A finite-volume particle method for compressible flows,” Mathematical Models and Methods in Applied Sciences, vol. 10, no. 9, pp. 1363-1382, 2000.

[2] R. Keck, “The finite volume particle method: A meshless projection method for incompressible flow,” Ph.D. thesis, University of Kaiserslautern, 2002.

[3] D. Teleaga, “A finite volume particle method for conservation laws,” Ph.D. thesis, University of Kaiserslautern, 2005.

[4] N. J. Quinlan, L. Lobovský, R. M. Nestor, “Development of the meshless finite volume particle method with exact and efficient calculation of

interparticle area," Computer Physics Communications, vol. 185, no. 6, pp. 1554-1563, 2014.

[5] D. Le Touzé, A. Colagrossi, G. Colicchio, M. Greco, "A critical investigation of smoothed particle hydrodynamics applied to problems with free-surfaces," International Journal for Numerical Methods in Fluids, vol. 73, no. 7, pp. 660–691, 2013.

[6] R. M. Nestor, M. Basa, M. Lastiwka, N. J. Quinlan, "Extension of the finite volume particle method to viscous flow," Journal of Computational Physics, vol. 228, no. 5, pp. 1733–1749, 2009.

[7] E. Jahanbakhsh, C. Vessaz, A. Maertens, F. Avellan, "Development of a Finite Volume Particle Method for 3-D fluid flow simulations," Computer Methods in Applied Mechanics and Engineering, vol. 298, pp. 80–107, 2016.

[8] R. Xu., P. Stansby, D. Laurence, "Accuracy and stability in incompressible SPH (ISPH) based on the projection method and a new approach. Journal of Computational Physics, vol. 228, no. 18, pp. 6703–6725, 2009.

[9] S. J. Lind, R. Xu, P. K. Stansby, B.D. Rogers, "Incompressible smoothed particle hydrodynamics for free-surface flows: a generalised diffusion-based algorithm for stability and validations for impulsive flows and propagating waves," Journal of Computational Physics, vol. 231, no. 4, pp. 1499–1523, 2012.

[10] A. Skillen, S. Lind, P. K. Stansby, B. D. Rogers, "Incompressible Smoothed Particle Hydrodynamics (SPH) with reduced temporal noise and generalised Fickian smoothing applied to body-water slam and efficient wave-body interaction," Computer Methods in Applied Mechanics and Engineering, vol. 265, pp. 163–173, 2013.

[11] A. Mokos, B. D. Rogers, P. K. Stansby, "A multi-phase particle shifting algorithm for SPH simulations of violent hydrodynamics with a large number of particles," Journal of Hydraulic Research, vol. 55, no. 2, pp. 143-162, 2016.

[12] G. Oger, S. Marrone, D. Le Touzé, M. de Leffe, "SPH accuracy improvement through the combination of a quasi-Lagrangian shifting transport velocity and consistent ALE formalisms," Journal of Computational Physics, vol. 313, pp. 76-98, 2016.

[13] M. H. Moghimi, N. J. Quinlan, "Suppression of non-physical voids in the finite volume particle method," in *Advances of Smoothed Particle Hydrodynamics*: *Proceedings of the 2017 SPHERIC Beijing International Workshop*, *Beijing China*, *October 17-20, 2017*, M. Liu, C. Huang, Eds. Beijing: ScienTech Publisher, 2017. pp. 177-183.

[14] L. Lobovský, E. Botia-Vera, F. Castellana, J. Mas-Soler, A. Souto-Iglesias, "Experimental investigation of dynamic pressure loads during dam break," Journal of Fluids and Structures vol. 48, pp. 407-434, 2014.